Polarization dependence of the magnetic fluctuations in Cr below T_N

P. Böni
Laboratory for Neutron Scattering ETH & PSI, CH-5232 Villigen PSI, Switzerland

B. J. Sternlieb and G. Shirane
Brookhaven National Laboratory, Upton, New York 11973

B. Roessli*
Institut Laue Langevin, F-38042 Grenoble, France

J. E. Lorenzo
Laboratoire de Crystallographie, CNRS, F-38042 Grenoble, France

S. A. Werner
Department of Physics, University of Missouri, Columbia, Missouri 65211
(Received 2 September 1997)

We have investigated the magnetic excitations in single-**Q**, single-domain Cr below T_N using polarization analysis of inelastically scattered neutrons for energy transfers up to 18 meV. The results show that the longitudinal (L) magnetic modes are enhanced below $\simeq 8$ meV with respect to the transverse (T) modes at low temperature. The latter are independent of the polarization with respect to the ordering vector $\mathbf{Q}'_{\pm}$ in the transverse spin-density-wave phase, i.e., they are isotropic. The L and T modes are not affected by the spin-flop transition to the longitudinal spin-density-wave phase at $T_{sf}=121$ K indicating that the transition is due to anisotropies and that it is not an intrinsic feature of the spin-density wave. There are indications that the L modes have a less steep dispersion curve and are more damped than the T modes in accordance with the three-band model by Fishman and Liu. With increasing temperature the intensity from the T and L modes increases strongly at small E transfer and their E dependence becomes similar. In particular, the enhancement of the L modes with respect to the T modes vanishes. Significant inelastic scattering is present at the silent peak positions. It surpasses even the scattering at the allowed peak positions at large E transfers. We argue that the silent inelastic scattering is partly responsible for the ''commensurate'' scattering at the (100) position due to resolution effects and that the major cross section at (100) is due to the longitudinally polarized Fincher-Burke mode at 4.2 meV. [S0163-1829(98)06502-3]

I. INTRODUCTION

Pure Cr is one of the most interesting itinerant antiferromagnets.[1] At the Néel temperature $T_N=311$ K, Cr undergoes a second-order phase transition to a transversely polarized spin-density-wave (TSDW) phase[2] characterized by an incommensurate wave vector $\mathbf{Q}'_{\pm}=(1\pm\delta'00)$, where $\delta'\simeq 0.048$ (Fig. 1). At the spin-flop temperature $T_{sf}=121$ K a first-order transition to a longitudinal spin-density-wave (LSDW) phase occurs, where the moments are oriented parallel to $\mathbf{Q}'_{\pm}$.[3] As a result of the cubic symmetry of paramagnetic Cr, three types of domains are present along the three [100] directions giving rise to six magnetic satellites around the (100) position in reciprocal space (H point). The incommensurate state is explained by the nesting properties of the electron and hole Fermi surfaces at the Γ and H points, respectively.[4]

The magnetic excitations of metallic Cr exhibit many unusual features due to the itinerant nature of the conduction electrons. In the LSDW phase, excitations with longitudinal (L) and transverse (T) polarization with respect to the ordered moment **m** emerge from the satellite positions with an extremely steep dispersion. The mode velocity is of the order of 1020 meV Å.[5] Below $E=8$ meV, the longitudinal modes, are enhanced.[6,7] This conclusion has very recently been confirmed by polarized neutron scattering and it has been shown that above 8 meV the excitations are isotropic.[8]

In a recent calculation using the random-phase approximation (RPA) Fishman and Liu have identified the longitudinal modes as phason modes, that occur due to the translational invariance of the incommensurate spin-density wave.[9] The transverse modes are usually termed spin waves, although they may be more complex than the spin-wave excitations in a conventional magnet. The RPA model also predicts that the phason mode velocity c_L is smaller than the spin-wave velocity c_T, resulting in a magnetic peak around 60 meV at the (100) position that has been observed recently by Fukuda *et al.*[10] The transverse modes have a velocity $c_T=\sqrt{3}v_F$, where v_F is the Fermi velocity that is independent of temperature, whereas the velocity of the phason modes c_L is smaller than c_T at low temperature and approaches c_T at T_N.[9] In addition, the longitudinal modes are supposed to be damped in contrast to the transverse modes.

A comparison of E scans at the $(1-\delta'00)$ and $(\delta'10)$ satellite positions using unpolarized neutrons indicated that the magnetic scattering in the TSDW phase may be enhanced

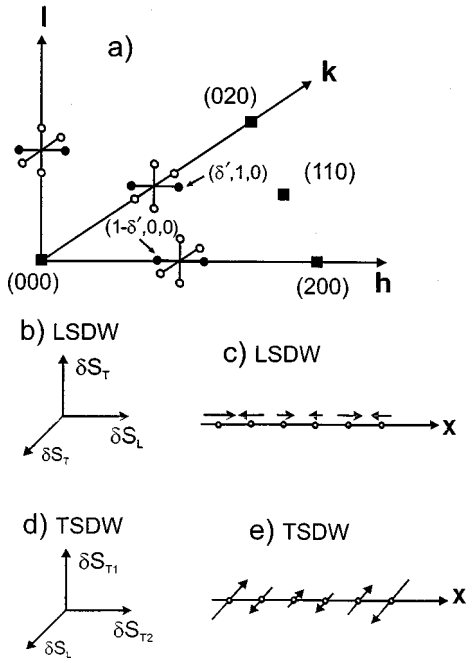

FIG. 1. (a) Reciprocal lattice of bcc Cr. The squares and circles represent chemical Bragg peaks and magnetic satellites, respectively. The filled circles indicate the allowed (not necessarily visible) satellites in the single-**Q** state, the open circles indicate the silent satellites. (b) Definition of the polarization directions of the transverse mode T and the longitudinal mode L in the LSDW phase. (c) Schematics of a single-**Q** LSDW. (d) Definition of the polarization directions of the T_1, T_2, and L modes in the TSDW phase. (e) Schematics of a single-**Q**, single-domain TSDW.

too below 1.2 meV at a temperature of 145 K.[6] However, it was not clear if the enhancement is caused by magnetic fluctuations along the ordering vector $\mathbf{Q}'_{\pm}$ (transverse to **m**, T_2 mode) or along **m**, that is conventionally called a longitudinal (L) mode (see Fig. 1). We denote the other transverse mode, which is perpendicular to $\mathbf{Q}'_{\pm}$ and **m** as T_1 mode. The T_1 and T_2 modes may be called spin waves. As we shall explain below, polarization analysis is necessary in order to discriminate between the different modes.

In addition to the incommensurate magnetic scattering, Fincher and co-workers[11] reported the occurrence of a well-defined excitation at the commensurate (100) position at $\simeq 4$ meV. This excitation was first believed to be discrete and was explained in terms of fluctuating blocks of spins.[11] Measurements with polarized neutrons showed, however, that the excitation has spin-flip character, being inconsistent with the model.[12]

Later measurements by Burke and co-workers[6] demonstrated that the scattering was due to excitations that follow linear dispersion curves originating from the $(1 \pm \delta' 00)$ satellite positions. Because the velocity of these branches was similar to the sound velocity for the $[\zeta 00]$ longitudinal acoustic phonon,[13] Burke and co-workers[6] proposed that the scattering might be due to magnetoelastic scattering. This interpretation was also thought to be unlikely because no other magnetovibrational scattering was observed and the temperature dependence of the intensity was not compatible with magnetoelastic scattering.[12] Moreover, it was shown that the symmetric branches with $\mathbf{Q} < \mathbf{Q}'_{-}$ and $\mathbf{Q} > \mathbf{Q}'_{+}$ are not present.[14] A proper understanding of these so-called Fincher-Burke modes is still missing.

TABLE I. Resolution parameters for the polarized beam setup. q_l, q_t, and q_z are the longitudinal, transverse, and vertical Q resolutions (FWHM) with respect to momentum transfer **Q**, respectively. ΔE is the energy resolution.

Mosaic	q_l	q_t	q_z	ΔE
0.00°	0.030 Å^{-1}	0.27 Å^{-1}	0.09 Å^{-1}	2.8 meV
0.73°	0.030 Å^{-1}	0.28 Å^{-1}	0.10 Å^{-1}	2.8 meV

Beside the well-defined Fincher-Burke modes, broad commensurate scattering occurs at the H point that increases strongly with increasing T near T_N.[11,15,10] An elegant explanation for this scattering was suggested by Sternlieb *et al.*, who found that at an energy scale of 0.5 meV, critical magnetic scattering evolves at all magnetic satellites very near T_N, causing a concommitent increase of the commensurate magnetic scattering at the H point.[16] At present it is not known if this explanation is also true for the commensurate scattering at higher energy.

The scope of the present work is an investigation of the inelastic magnetic scattering in single-**Q**, single-domain Cr using polarized neutrons to discriminate between the different magnetic modes in the LSDW and TSDW phases. A short account of the present work has been given elsewhere.[17] We shall demonstrate that the longitudinal fluctuations are enhanced below and above the spin-flop temperature T_{sf}. In particular, we show that within experimental accuracy the energy dependence of the L and T modes is identical below and above T_{sf}, respectively. Close to T_N, the energy dependence of the magnetic scattering looks different at the allowed and the silent satellite positions. Finally, it is shown that the major contribution at the commensurate position is due to the Fincher-Burke mode at 4 meV that is longitudinally polarized.

II. EXPERIMENTAL

The neutron-scattering experiments were performed on the triple axis spectrometer IN20 at the Institut Laue Langevin in Grenoble. The neutrons were polarized and analyzed by means of Heusler (111) using a fixed final energy $E_f = 14.7$ meV. The horizontal collimations were 40-60-120-open from before the monochromator to the detector. Typical resolution parameters are given in Table I. We point out that the coarse transverse Q resolution q_t is mostly due to the coarse collimation of the spectrometer and not due to the mosaicity of the sample. Higher-order neutrons were suppressed by means of a pyrolytic graphite filter installed before the analyzer. A flat coil spin flipper was placed before the analyzer. The flipping ratio as measured at the $(\delta' 1\ 0)$ satellite position in the LSDW phase was $R = 15$ (Fig. 2).

The Cr crystal used for the experiment (Cr#10) was an irregularly shaped 25.6 g single crystal with a mosaic of 0.73°.[16] Prior to the measurements the crystal was cooled through the Néel temperature $T_N = 311$ K in a magnetic field $B_{[100]} = 20$ T in order to induce a single-**Q** state with $\mathbf{Q}'_{\pm}$ along the [100] direction (Fig. 1). However, as the magnetic moments associated with $\mathbf{Q}'_{\pm}$ in the transverse phase are per-

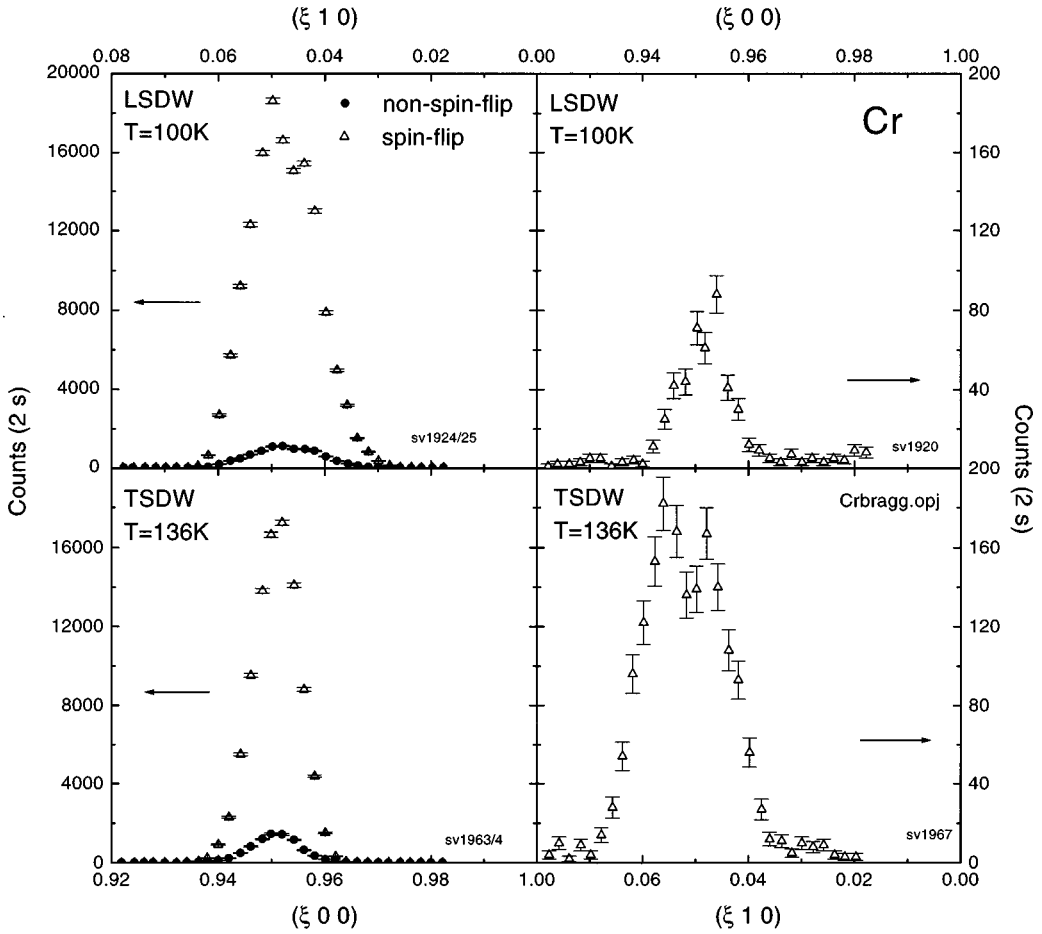

FIG. 2. Top: Elastic scans at the allowed and silent satellite positions $(-\delta' 10)$ and $(1-\delta' 00)$ in the LSDW phase. Bottom: Elastic scans at the allowed and silent satellite positions $(1-\delta' 00)$ and $(-\delta' 10)$ in the TSDW phase. The measurements demonstrate the excellent single-**Q**, single-domain configuration of the sample in a field of 4 T.

pendicular to $\mathbf{Q}'_{\pm}$, there exist two magnetic domains with the moments oriented along [010] and [001]. Therefore, the longitudinal (L) and the transverse T_1 mode cannot be separated with unpolarized neutrons. In the LSDW phase, however, this problem does not arise because the transverse modes are degenerate.

In order to enforce a single-domain structure in the TSDW phase we have mounted the sample on the cold finger of a superconducting cryomagnet and applied a vertical field $B_{[001]}=4$ T that aligns the magnetic moments along the $[010]$ direction. With a polarized beam, the intensities given in Table II can be determined for the spin-flipper off (non-spin-flip scattering) and on (spin-flip scattering), respectively.

In principle, a distinction between the different modes can also be achieved by performing measurements in zero and in high field and by using the property that only spin fluctuations normal to the scattering vector **Q** contribute to the neutron-scattering cross section. Then, the different modes can be disentangled by calculating the appropriate differences between the cross sections at the different allowed satellite positions.[18] However, the analysis is more difficult than with polarization analysis.

TABLE II. Polarization and selection rules for the magnetic fluctuations and magnetic satellite peaks in single-domain Cr. **Q** is the scattering vector.

Phase	**Q**	Satellite	Non-spin-flip	Spin-flip
Longitudinal SDW	$(1\pm\delta' 00)$	Forbidden	T	T
	$(\pm\delta' 10)$	Allowed	T	L
Transverse SDW	$(1\pm\delta' 00)$	Allowed	T_1	L
	$(\pm\delta' 10)$	Forbidden	T_1	T_2

Figure 2 shows that the silent reflections in the LSDW phase $(1-\delta' 0,0)$, and in the TSDW phase $(\delta' 1\ 0)$ are more than a factor of 100 smaller than the allowed reflections, proving the excellent single-**Q** structure of our sample in both phases. The flipping ratio $R\simeq 11$ at the allowed position in the TSDW phase indicates that the sample is essentially in a single-domain state. We note that allowed peaks can only be observed, if $\mathbf{m}\perp\mathbf{Q}$ because of the selection rule for magnetic scattering.

III. RESULTS

Figure 3 shows measurements of the transverse and longitudinal modes at $(\delta' 1\ 0)$ $(\delta'=0.048)$ in a field $B_{[001]}=4$ T that demonstrate how well the L and T modes can be separated in the LSDW phase at $T=100$ K. The results confirm that the L modes are enhanced below 8 meV when compared with the T modes, in agreement with previous

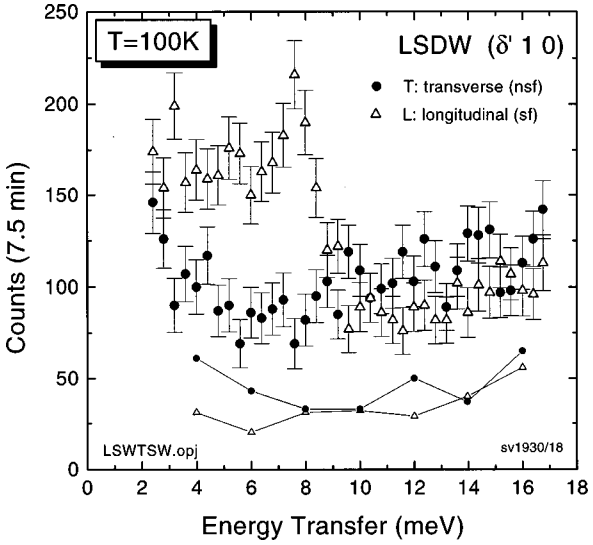

FIG. 3. Longitudinal and transverse fluctuations as measured in the LSDW phase at $T=100$ K. Below 8 meV the scattering is enhanced. The measurements were conducted in a vertical field of 4 T. The background is indicated by the solid lines for spin-flip (open triangles) and non-spin-flip (filled circles) scattering.

unpolarized[6,7] and polarized neutron[8] measurements. A comparison with data taken at $B_{[001]}=0.1$ T proved that the magnetic fluctuations are not affected by a field of 4 T. This was expected because the energy scale of the magnetic field $E_H \simeq 0.3$ meV is much smaller than the probed energy transfers. The background has been obtained by measuring the intensity at $(2^{-1/2}2^{-1/2}0)$ for spin flipper off and on and is indicated in Fig. 3 and the following figures by solid lines. The background is of the order of 37 counts/7.5 min and is almost independent of polarization, except at small E transfer.

In a next step we have conducted constant **Q** scans at the satellite positions $(1\text{-}\delta'\,0\,0)$ and $(\delta'\,1\,0)$ $(\delta'=0.048)$ in the TSDW phase at $T=136$ K in order to discriminate between the three different modes T_1, T_2, and L (Fig. 1). Figure 4 shows that the longitudinal fluctuations are enhanced below $E\simeq 8$ meV, when compared with the transverse T_1 mode, similarly as in the LSDW phase. The intensities of the T_1 and T_2 modes are identical and independent of E within the measured energy window as expected for an isotropic antiferromagnet.

The direct comparison of the longitudinal (Fig. 5) and the transverse scattering in the LSDW and TSDW phase shows that the cross sections are identical within the experimental accuracy. The distinct, resolution-limited peak at 7.6 meV appears in both phases. It is much more pronounced in the present work because the L mode and T modes are not superimposed as in multidomain samples. The cross sections have only been corrected for the finite flipping ratio ($R=15$) and for the nonperfect single-domain state ($R_{sf}=11$) in the LSDW and TSDW phase, respectively. The thermal population factors $\langle n+1\rangle = 1/[1-\exp(-E/k_BT)]$ enhance the data at 136 K by roughly 20% with respect to the data at 100 K. This effect essentially cancels the 10% increase of the intensity observed at $(\delta'1{,}0)$ when compared with $(1\text{-}\delta'\,0\,0)$ (see Figs. 2 and 4).

With increasing temperature, the L and T modes approach each other. Figure 6(a) shows constant **Q** scans at the allowed satellite $(1\text{-}\delta'\,0\,0)$ at $T=299$ K $(=0.96T_N)$. The data indicates that the enhancement of the L mode below 8 meV has vanished or moved to such a small E that it could not be observed anymore. The magnetic scattering is strongly enhanced for small E transfers.

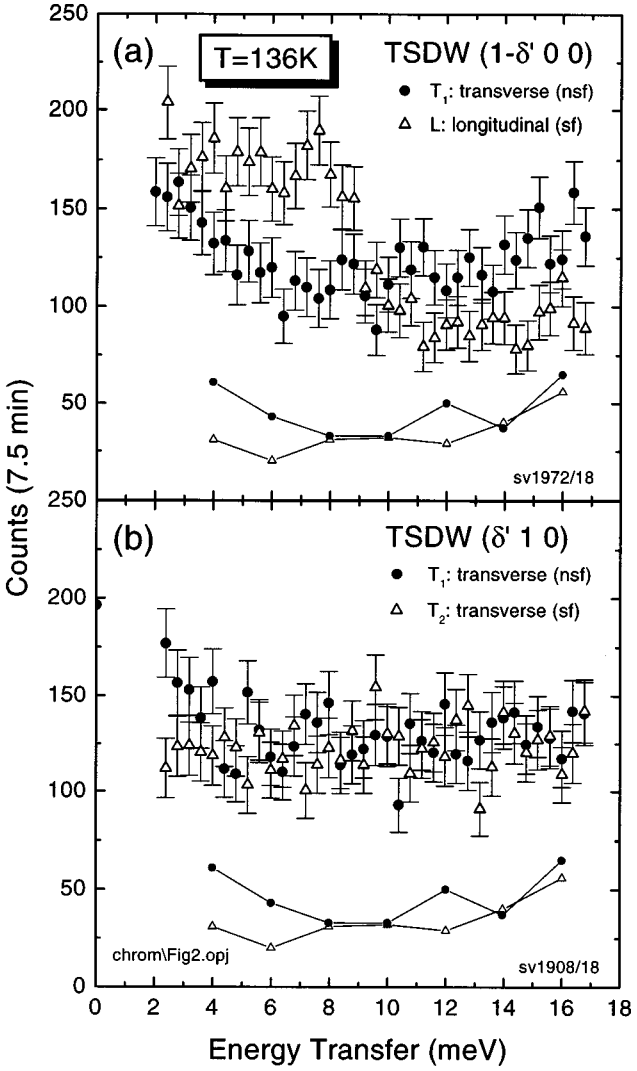

FIG. 4. (a) Measurement of the L and T_1 modes in the TSDW phase at $T=136$ K. L is enhanced below 8 meV. (b) The transverse modes T_1 and T_2 are independent of the polarization with respect to $\mathbf{Q}'_{\pm}$. The background is indicated by the solid lines.

The measurements at $(\delta'\,1\,0)$ confirm again [Fig. 6(b)] that the T_1 and T_2 modes are identical as expected. The E dependence of the scattering cross section is, however, different from (a) because of the combined effects of a coarse transverse Q resolution, $q_t=0.28$ Å^{-1} [full width at half maximum (FWHM)] (see Table I), caused by the coarse collimation and a smaller incommensurability $\delta'=0.040$ $(\equiv 0.087$ Å$^{-1})$ at $T=299$ K. Therefore we pick up inelastic intensity from the magnetic scattering at (010) that grows significantly near T_N.[15]

We have also conducted inelastic scans at the silent satellite positions $(01\text{-}\delta'\,0)$ and $(1\,\delta'\,0)$ (Fig. 7). We use the same notation for the polarization of the modes as we did for the allowed scattering, although there is no ordered moment at the silent satellite positions that defines a reference sys-

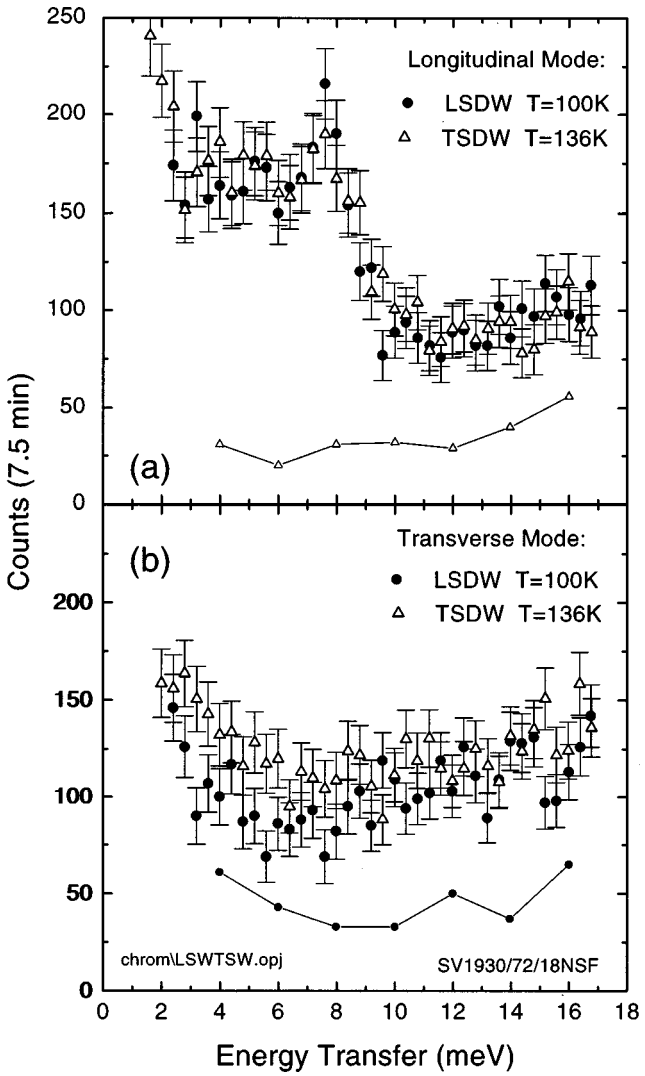

FIG. 5. Comparison of the longitudinal scattering in the LSDW and TSDW phase. The data have only been corrected for the finite flipping ratios. The background is indicated by the solid lines.

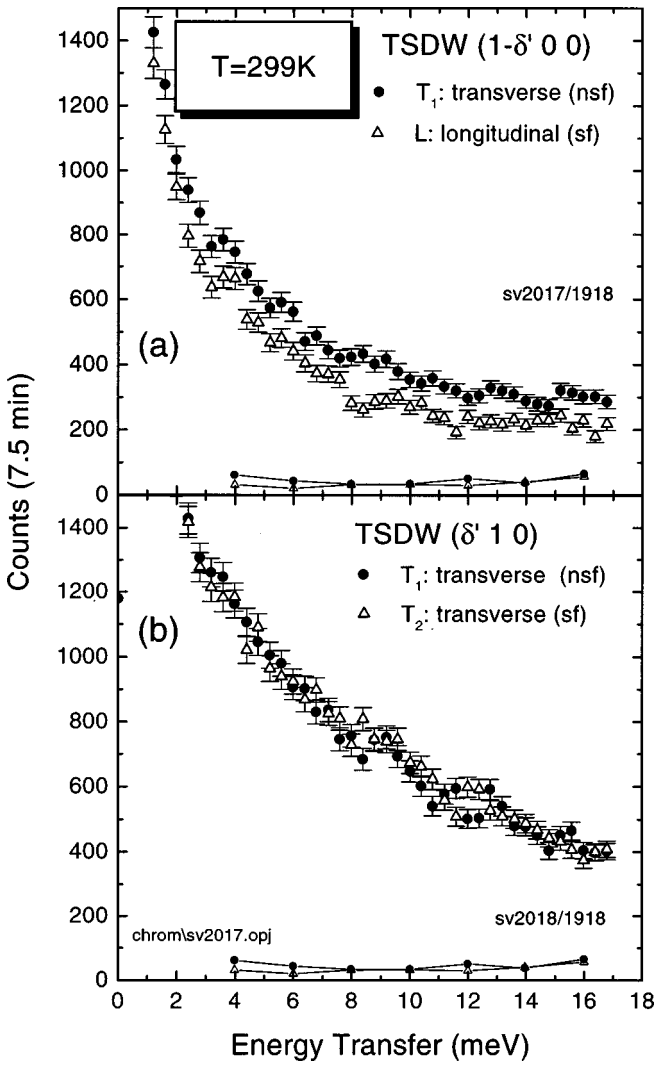

FIG. 6. (a) Measurement of the L and T_1 mode in the TSDW phase at $T=299$ K at the allowed satellite peaks. The overall shape of the L and T scattering becomes identical. (b) The transverse modes T_1 and T_2 are also identical. The background is indicated by the solid lines.

tem. The data show that there is a significant magnetic response over the whole E range investigated. In fact, at large E, the intensity is even larger than at the allowed satellite peaks. The L and T_1 modes are identical. However, they are essentially independent of E in contrast to the scattering at the allowed peaks. In particular, the signal does not increase with decreasing E, indicating that the modes do not contribute yet (if they do) to the phase transition.

The measurements at $(1\,\delta'0)$ are significantly contaminated by the commensurate magnetic scattering at (100) due to the coarse transverse Q resolution discussed above. In particular, at $E\simeq 4.5$ meV even the Fincher-Burke mode becomes visible (see below). The large inelastic intensity at the silent satellites is remarkable because at this temperature the reported enhancement of the inelastic scattering at 0.5 meV at the silent satellite peaks is still small.[16]

Finally, we have investigated the polarization dependence of the commensurate magnetic scattering near 4 meV at the (100) position (Fig. 8). We find an enhancement of the intensity of the L mode near 4.2 meV that can be identified as Fincher-Burke mode.[6,11] The transverse scattering T_1 is independent of energy. Similar measurements at (010) show that the two modes T_1 and T_2 are identical.

The constant E measurements in Fig. 9 confirm the results of Pynn and co-workers[12] that the Fincher-Burke mode has a longitudinal polarization. Our data are, however, much cleaner because of the excellent single-domain state obtained in a smaller applied magnetic field. The peaks at the $(1\pm\delta'00)$ positions correspond to cuts through the rods of inelastic scattering that emerge from the magnetic satellites (see insert of Fig. 9).

The interpretation of the broad commensurate peak in the T_1 scattering is not trivial. The constant Q scan in Fig. 8 shows that there is appreciable scattering at all E transfers and it is remarkable how well the E profile of the T_1 mode resembles the scattering at the silent peaks (Fig. 7). We interpret the broad peak to be mostly due to the inelastic scattering at the silent satellites that gives rise to strong magnetic scattering at the (100) position because of the coarse Q resolution as discussed by Sternlieb *et al.*[16] Note that $\delta'=0.040$ corresponds to 0.087 Å^{-1} that is comparable to the half width at half maximum of the transverse and vertical Q

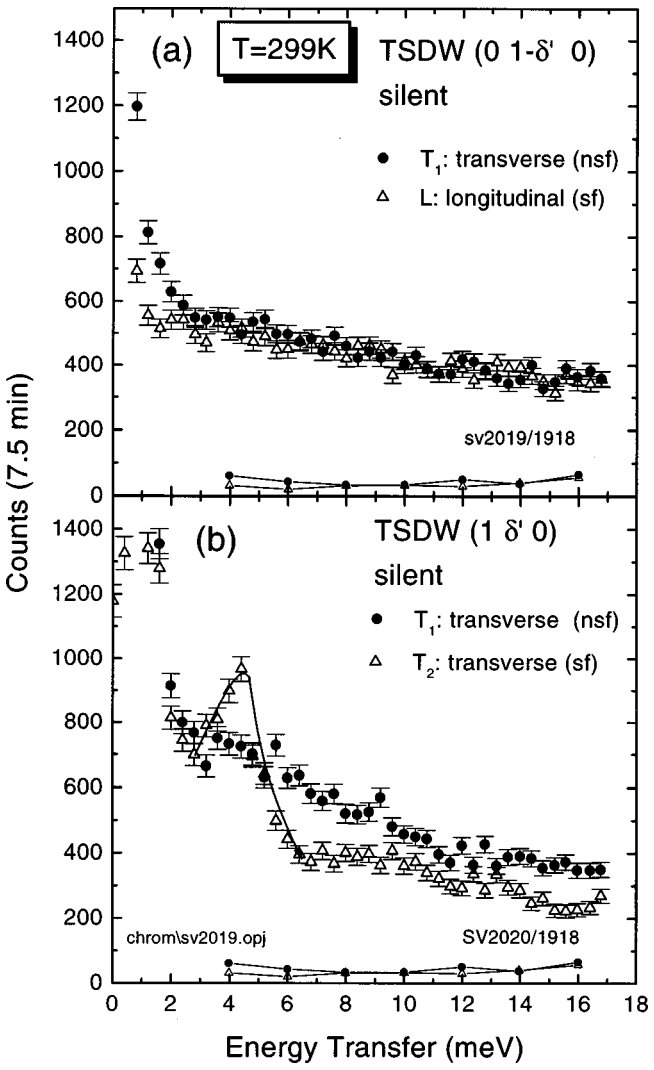

FIG. 7. Measurement of the L, T_1, and T_2 mode in the TSDW phase at $T=299$ K at the silent satellite peak positions. The L and T modes become identical and are essentially independent of E. The data at $(1\delta'0)$ are seriously contaminated by the commensurate scattering at (100) due to the coarse Q resolution. The background is indicated by the solid lines.

resolutions q_t and q_v, respectively, (Table I). Note, that four silent satellites contribute to the scattering at (100).

In contrast, the magnetic scattering at the allowed satellites $(1\pm\delta'00)$ shows a strong E dependence (Fig. 6). It does not contribute to the commensurate scattering because of the good longitudinal resolution q_l. As a consequence, the broad ''commensurate'' peak may also explain the distortion of the scattering at the allowed $(\delta'10)$ satellite via the coarse transverse Q resolution given by q_t in Table I [Fig. 6(b)].

In order to obtain more quantitative information about the commensurate scattering, we have fitted the constant E data at $E=4.2$ meV of the transverse scattering (Fig. 9) using three Gaussians. The fitted parameters are given in Table III. The inelastic incommensurate scattering that emanates from the $(1\pm\delta'00)$ satellites is resolution limited in Q because of the very steep rise of the dispersion curves.

The longitudinal inelastic data in Fig. 9 were fitted using four Gaussians, keeping the parameters of one of them fixed at the values obtained for the broad component of the T_1

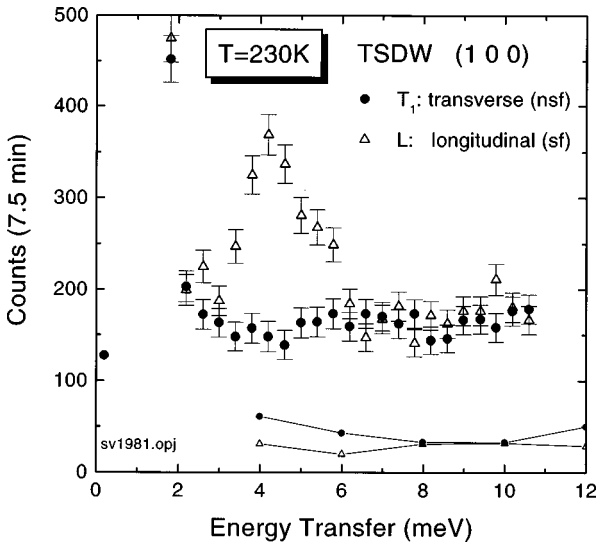

FIG. 8. Longitudinal and transverse cross sections at the commensurate (100) position in the TSDW phase at $T=230$ K. The background is indicated by the solid line.

scattering. The resulting fitting parameters for the remaining three Gaussians are also given in Table III.

The least-square fits show that the rods due to the L modes are indeed broader than the resolution limited rods of the T modes. Moreover, the L rods are closer to (100) indicating, that the longitudinal scattering might be responsible for the bending of the cones of inelastic intensity towards (100) as observed with scattering experiments using unpolarized neutrons.[11,15,10] A linear extrapolation of the shift of the L modes at 4.2 to 30 meV would yield peaks near 0.98 and 1.02 at 30 meV. The broadening of the L peaks with respect to the T peaks is compatible with the predictions of Fishman and Liu[9] that (i) the velocity c_L of the longitudinal modes is smaller than the velocity c_T of the transverse modes (below T_N) and that (ii) the longitudinal modes are damped. The difference in dispersion for the L and T modes may make it difficult to resolve the spin waves in Cr with unpolarized neutrons.

The effect of the L modes of having a smaller c_L and a damping is a smearing of the cross section in Q and E space at larger E transfers, resulting in a reduced intensity from the longitudinal modes above 14 meV when compared with the transverse modes (see Fig. 4). This conjecture must be confirmed with more detailed measurements and careful determinations of the background.

IV. DISCUSSION

Our measurements provide a clear distinction between the transverse and longitudinal modes that occur in the LSDW and TSDW phase of single-domain Cr. The results show that within experimental uncertainty, the L and the T modes do not change at the spin-flop temperature T_{sf}, indicating that this transition is not related to the itinerant features of the spin-density wave. This is expected because the band energies are much larger than anisotropy energies in isotropic systems. In addition, between $E\simeq 8$ and 18 meV, the L and T modes are essentially isotropic. There is, however, an indication that the T mode is stronger than the L mode. This

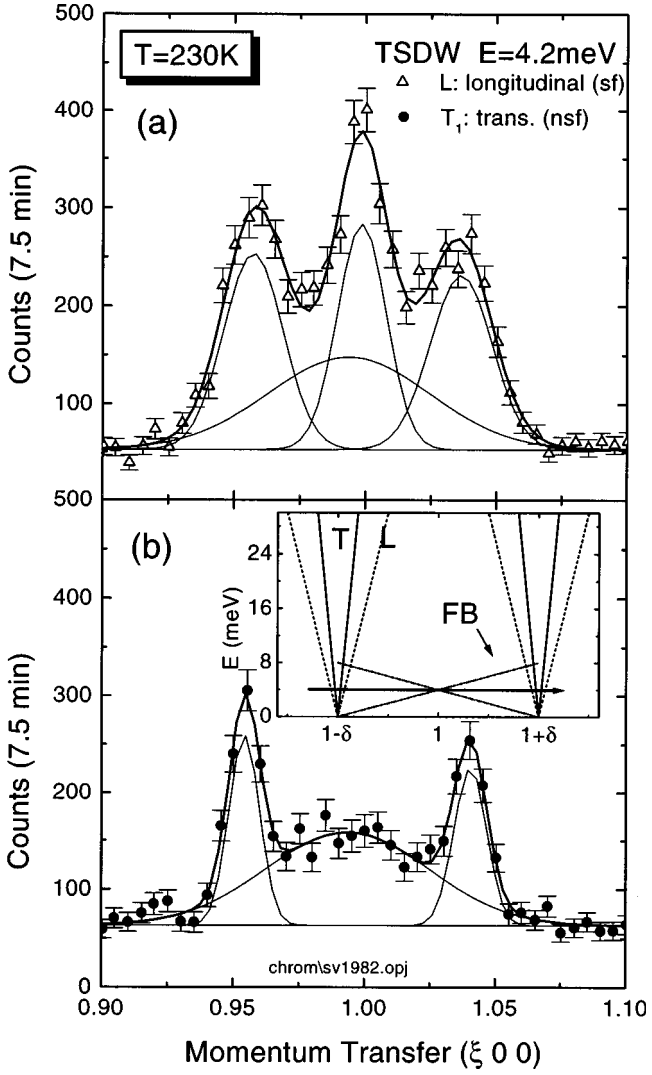

FIG. 9. Constant E scans at 4.2 meV probing the longitudinal and transverse fluctuations along the [100] direction in the TSDW phase at $T=230$ K. The background is indicated by the horizontal solid line. The insert shows the intersection of the constant E scan with the dispersions of the transverse (solid lines) and the longitudinal modes (broken lines) as well as the Fincher-Burke modes (FB).

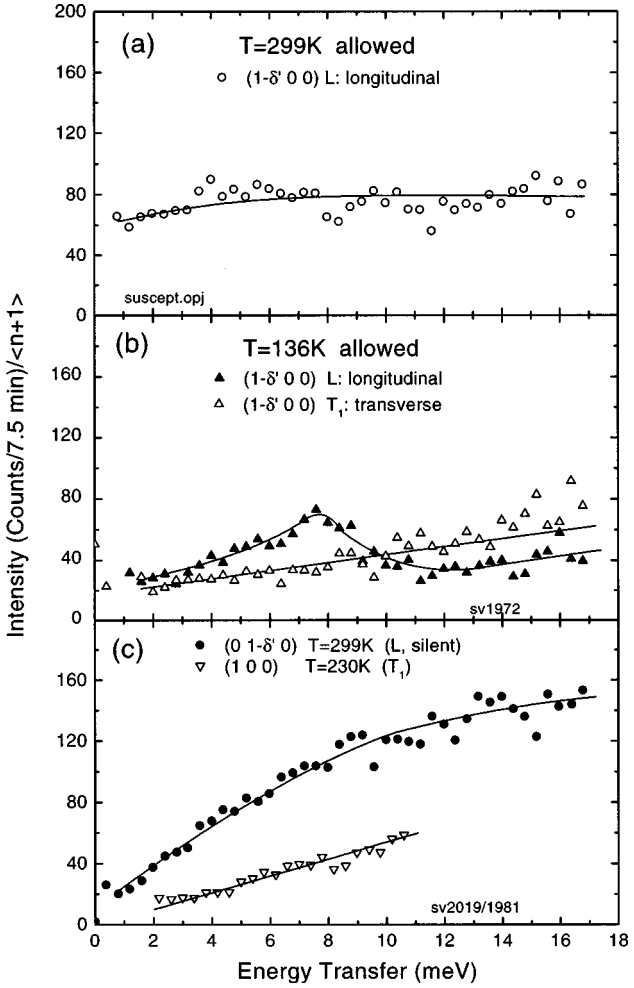

FIG. 10. Thermally corrected constant **Q** peak intensities for different temperatures and positions in the reciprocal space. Note the large intensity at the silent position when compared with the intensity at the allowed position. The E dependence of the silent scattering evolves in a similar way as the commensurate scattering.

may be reconciled with the prediction of Fishman and Liu[9] that the L modes have a lower velocity than the T modes at this temperature. At $0.96T_N$, the modes become identical, in particular the enhancement of the longitudinal scattering at $E<8$ meV has vanished.

In Fig. 10 we have plotted the thermally corrected magnetic cross sections for $T=136$ and 299 K after subtracting the background. The spectra look very similar as the corresponding ones reported by Lorenzo *et al.*[7] in the LSDW phase. The top graph (a) indicates clearly that the dynamical susceptibility $\chi(Q,\omega)$ at 299 K is enhanced at all E transfers when compared with 136 K (b). This effect is most likely related to the proximity of T_N and the occurrence of critical scattering and cannot be treated within the framework of the random-phase approximation of Ref. 9. The concomitant increase of the L and T modes (see Fig. 6) indicates that both modes are responsible for the phase transition to the para-

TABLE III. Fit parameters (in reciprocal lattice units) for constant E scans assuming Gaussian peaks. The longitudinal instrumental resolution is given in reduced units by $\Delta\zeta=2\pi q_l/a=0.015$ ($a=2.88$ Å^{-1}). The broad Gaussian at 0.994 of the transverse scattering has been kept fixed during the fitting of the longitudinal scattering.

Mode	Position	Width	Position	Width	Position	Width
Transverse (T_1)	0.9542	0.014	0.994	0.075	1.0405	0.015
scattering ($\chi^2=0.73$)	±0.0004	±0.001	±0.003	±0.009	±0.0005	±0.001
Longitudinal (L)	0.9572	0.027	0.9985	0.022	1.0364	0.028
scattering ($\chi^2=1.15$)	±0.0008	±0.002	±0.0007	±0.002	±0.0010	±0.002

magnetic phase. The strong increase of the transverse intensities is difficult to reconcile with the predicted nonrenormalization of the T modes,[9] i.e., according to the three-band model c_T should remain constant and the transverse modes should not be damped.

Figure 10(c) demonstrates that the thermally corrected intensity at the silent satellite position (filled circles) is larger for $E>8$ meV than the intensity at the allowed satellite (a). We note that our assignment of polarizations to the scattering occurring at the silent positions according to the allowed magnetic satellites is arbitrary, since there is no preferred moment direction defined at the silent peaks with the exception of nonaligned domains. Therefore, it is not surprising that the L and the T modes are identical since they simply represent electron-hole excitations that are enhanced due to the nesting properties of the Fermi surface.

The interpretation of the commensurate peak has a long history. Mikke and Jankowski[19] and Fincher and co-workers[11] have observed a strong increase of the intensity near (100). Recently, Fukuda *et al.* have measured the commensurate scattering up to higher E and interpret the increase of the scattering with increasing E and T in terms of the commensurate scattering being an intrinsic property of Cr.[10] Based on our data we propose another explanation: At least up to 18 meV our data is consistent with the idea that the inelastic scattering from the four silent peaks is responsible for the increase of the magnetic intensity at (100). The intensity is expected to increase due to (i) the increase of $\langle n+1\rangle$ with increasing T and (ii) the increasingly worse resolution of the spectrometer with increasing E.

Taking all the above results together we end up with the following conclusions. Inelastic magnetic scattering in the ordered phases of Cr occurs at the allowed and silent incommensurate magnetic satellite positions. It is almost isotropic above $E=8$ meV. The scattering at the silent positions is most likely due to excitations between the electron and hole Fermi surface at the Γ and (100) points, respectively. The excitations are concentrated at the silent peaks ($\mathbf{Q}_{\pm}$) because of the nesting properties of the Fermi surface and may be explained in terms of a two-band model.[20]

In order to understand the spin dynamics around the allowed satellites, Fishman and Liu have proposed the three-band model.[9] According to this model, the actual wave vectors of the spin-density wave, $\mathbf{Q}'_{\pm}$ are given by $(G/2)(1-\delta'00)$, where $0<\delta'<\delta$ and $G/2=2\pi/a$. Here, the mismatch δ reflects the nesting of the bare electron and hole Fermi surfaces that are not distorted by the spin-density wave. If we identify the essentially isotropic incommensurate scattering as electron-hole excitations, then it is expected that the scattering at the silent positions and the allowed positions is different at low E transfers (as probed in our experiments), because the nesting parts of the Fermi surface for the silent and allowed peaks are different.

The enhancement of the longitudinal scattering below 8 meV occurs only at the allowed satellite positions. Therefore it must be an effect of the rearrangement of the Fermi surface due to magnetic ordering (see Fig. 1 in Ref. 9). One may tentatively interpret the enhanced part[21] of the longitudinal scattering as collective excitations that are responsible for the long-range magnetic order below T_N. Therefore, $\Delta=8$ meV may be identified as a characteristic energy that provides a gap for electron-hole excitations at $q=0$. In an itinerant ferromagnet, Δ would correspond to an exchange splitting. As soon as the excitations of the enhanced part of the L modes intersect the sea of electron-hole excitations near 8 meV, they become strongly damped and vanish. With increasing temperature Δ decreases, finally leading to the disappearance of the enhanced part of the L modes and the loss of magnetic order. Very close to T_N, critical scattering evolves with longitudinal and transverse polarization, similarly as in itinerant ferromagnets like Ni.[22] The stronger damping of the low-energy L modes, when compared with the T_1 modes (see Fig. 9) may be explained by the interaction of the enhanced part of the L modes with electron-hole excitations from the nonenhanced isotropic part of the L and T modes. It seems to be important to investigate the L and T_1 modes below 10 meV in more detail using polarization analysis in order to characterize their evolution with T, i.e., their dispersion and damping.

The only commensurate scattering that we have observed unambiguously is the longitudinally polarized Fincher-Burke mode[11,6] that has been identified many years ago at (100) near 4 meV (Fig. 9). It follows linear dispersion curves that originate from the $(1\pm\delta'00)$ satellite positions.[6] Accordingly, the peak at 8 meV in Fig. 4 may be readily interpreted as Fincher-Burke mode at the incommensurate positions $1\pm\delta'$. However, to the best of our knowledge, this mode has not been observed in the LSDW phase at (100) (and 4 meV), although our data clearly shows that the peak at 8 meV is present in both phases (Fig. 5). Therefore, the excitation in the TSDW phase at 8 meV may not be related to the Fincher-Burke mode. A closer investigation of this behavior will be a subject of further investigations. Our present study does not provide any further clues on the physical mechanism of this mode.[14]

ACKNOWLEDGMENTS

We are grateful to Y. Endoh, R. Pynn, and R. Fishman for helpful discussions. In addition, we would like to thank J. Kulda for the help during setting up the experiment on IN20 at the ILL. Work at Brookhaven National Laboratory was supported by the Division of Materials Sciences, U.S. D.O.E., under Contract No. DE-AC02-76CH00016.

*Present address: Laboratory for Neutron Scattering ETH & PSI, CH-5232 Villigen PSI, Switzerland.

[1] E. Fawcett, Rev. Mod. Phys. **60**, 209 (1988).

[2] J. P. Hill, G. Helgesen, and Doon Gibbs, Phys. Rev. B **51**, 10 336 (1995).

[3] S. A. Werner, A. Arrott, and H. Kendrick, Phys. Rev. **155**, 528 (1967).

[4] F. W. Holroyd and E. Fawcett, J. Low Temp. Phys. **38**, 421 (1980).

[5] J. Als-Nielsen, J. D. Axe, and G. Shirane, J. Appl. Phys. **42**, 1666 (1971).

[6] S. K. Burke, W. G. Stirling, and K. R. A. Ziebeck, Phys. Rev. Lett. **51**, 494 (1983).

[7] J. E. Lorenzo, B. J. Sternlieb, G. Shirane, and S. A. Werner, Phys. Rev. Lett. **72**, 1762 (1994).
[8] Y. Endoh, T. Fukuda, K. Nakajima, and K. Kakurai, J. Phys. Soc. Jpn. **66**, 1615 (1997).
[9] R. S. Fishman and S. H. Liu, Phys. Rev. Lett. **76**, 2398 (1996); Phys. Rev. B **54**, 7252 (1996).
[10] T. Fukuda, Y. Endoh, K. Yamada, M. Takeda, S. Itoh, M. Arai, and T. Otomo, J. Phys. Soc. Jpn. **65**, 1418 (1996).
[11] C. R. Fincher, G. Shirane, and S. A. Werner, Phys. Rev. B **24**, 1312 (1981).
[12] R. Pynn, W. G. Stirling, and A. Severing, Physica B **180&181**, 203 (1992).
[13] W. M. Shaw and L. D. Muhlestein, Phys. Rev. B **4**, 969 (1971).
[14] B. J. Sternlieb, G. Shirane, S. A. Werner, and E. Fawcett, Phys. Rev. B **48**, 10 217 (1993).
[15] B. H. Grier, G. Shirane, and S. A. Werner, Phys. Rev. B **31**, 2892 (1985).
[16] B. J. Sternlieb, J. P. Hill, T. Inami, G. Shirane, W.-T. Lee, S. A. Werner, and E. Fawcett, Phys. Rev. Lett. **75**, 541 (1995).
[17] P. Böni, B. J. Sternlieb, B. Roessli, J. E. Lorenzo, G. Shirane, and S. A. Werner, Physica B (to be published).
[18] W. T. Lee, J. A. Fernandez-Bacca, R. S. Fishman, and S. A. Werner, Physica B (to be published).
[19] K. Mikke and J. Jankowski, J. Magn. Magn. Mater. **14**, 280 (1979).
[20] P. A. Fedders and P. C. Martin, Phys. Rev. **143**, 245 (1966).
[21] The longitudinal fluctuations may be decomposed into an isotropic part that resembles the T_1 modes and an enhanced part. The isotropic part is most likely due to electron-hole excitations, the enhanced part due to magnetic ordering.
[22] P. Böni, J. L. Martínez, and J. M. Tranquada, Phys. Rev. B **43**, 575 (1991).